INITIAL COMMISSIONING OF THE MAGNEX SPECTROMETER

A.Cunsolo[a,b], F.Cappuzzello[a,b,*], M.Cavallaro[a,b], A.Foti[b,c], A.Khouaja[a], S.E.A.Orrigo[a,b], J.S.Winfield[a], L.Gasparini[a,b], G.Longo[a,b], T.Borello-Lewin[d], M.R.D.Rodrigues[d], M.D.L.Barbosa[d], C.Nociforo[e], H.Petrascu[f]

a) INFN Laboratori Nazionali del Sud, Catania, Italy
b) Dipartimento di Fisica e Astronomia, Università di Catania, Italy
c) INFN Sezione di Catania, Catania, Italy
d) IFUSP, São Paulo, Brazil
e) GSI, Darmstadt, Germany
f) NIPNE, Bucharest, Romania
** Corresponding author, e-mail: cappuzzello@lns.infn.it*

Abstract: *The MAGNEX large-acceptance spectrometer was commissioned with beams from the LNS Tandem. The optics was tested with elastically scattered ^{7}Li, ^{16}O and ^{48}Ti beams with apertures mounted after the target. A demonstration of the particle identification capabilities of the PSD start detector and the focal plane detector was given by a measurement of the $^{19}F(^{7}Li,^{7}Be)^{19}O$ charge exchange reaction at 25° ± 5º. The charge state distribution of scattered ^{48}Ti ions was also measured and found to be in good agreement with predictions. Preliminary results of the software reconstruction of excitation energy and angles, which used matrices based on a 3D-interpolation of the measured field maps, are encouraging.*

1 INTRODUCTION

The MAGNEX large-acceptance spectrometer [1,2] was designed particularly for RNBs from the EXCYT facility at the LNS, although there are several advantages that carry over to experiments induced by stable beams from either the Tandem or SC cyclotron. The spectrometer relies partly on hardware (especially the shape of the entrance and exit dipole pole tips) and partly on software (ray reconstruction) to overcome the strong aberrations inherent in the 50-msr acceptance.

Apart from the final scattering chamber, the spectrometer was complete and ready for the first beam to target and scattered particles through to the focal plane in April 2005. The Focal Plane Detector (FPD) [3] continued to be tested with an α-source during the summer and was further tested with scattered beams from the LNS Tandem in December.

The spectrometer was ready for initial commissioning in February 2006. "Initial" because the small scattering chamber ("*Cameretta*") with a fixed exit angle port at 25º was used. Furthermore, the fields for the magnetic elements – Quadrupole, Dipole and α surface coils – were set according to estimated values rather than from those derived from the measured field maps. The β surface coil, for which the effect on the focal surface is rather complicated, was not energized in general, apart from a brief test to show that it did have some effect.

2 EXPERIMENTAL DETAILS

The optics in general, was tested with elastically scattered ^{16}O, ^{7}Li and ^{48}Ti beams on gold and nickel targets. Various apertures were mounted about 10 cm after the target, including one corresponding to the nominal 50-msr full acceptance and an aperture with a set of 1-mm holes. The microchannel-based start detector (PSD) described in ref. [3] was installed in a small chamber after the "*Cameretta*".
The FPD was fixed at a position roughly corresponding to the intermediate kinematic factor $K = -0.25$. Normally, the FPD should be moved closer to or further from the dipole exit, in order to compensate the kinematic shift of the focal plane for different reactions. However, since the remote control system for this movement was not finished, we decided to compensate changes in K by use of the αsurface coil.

2.1 FPD Parameters

Suitable isobutane gas pressures and proportional wire voltages were studied for the different heavy ions detected. The choice of gas pressure is essentially a compromise between producing enough primary electrons through ionization and minimizing the straggling of the ions passing through the detector. The anode wire voltages need to be sufficiently high to induce charges to produce signals above noise on at least three consecutive strips (pads), while keeping in the proportional regime. However, in practice the voltage is often limited by the saturation of the preamplifier for the energy-loss signal, which is taken from the wire. Some typical pressures and voltages used during the tests are given in Table 1.

Table 1: Typical FPD isobutane gas pressures and proportional and the silicon detector that triggered the event. The final wire voltages for various detected ions. "Energy" is after the scattering at 25º and after energy-loss in the PSD foil.

Ion	**Energy (MeV)**	**Pressure (mbar)**	**Voltage (V)**
^{7}Li	50	30	750
^{16}O	75	20	650
^{48}Ti	100	10	490

2.2 FPD counting rate and data acquisition dead time

With such a large gas-filled detector (dimensions 160 cm long, 25.5 cm tall, 50 cm deep), the acceptable counting rate to maintain good particle identification is mostly limited by the drift time of the electrons and the build up of positive ions ("space charge"). Since we have a rather long acquisition readout time (224 multiplexed signals must be processed by the VME CRAMS modules), the data acquisition dead time may also be significant. These two count-rate dependent parameters were measured by setting the spectrometer to detect the elastic scattering of ^{48}Ti on a gold target and, run by run, increasing the beam current. Table 2 gives the measured counting rate in the detector (the number of silicon detector triggers) and the resulting dead time of the acquisition system (the ratio of the number of accepted events to triggers). Only at the highest beam current studied, corresponding to a trigger rate of 1.75 kHz, was there a noticeable deterioration of the ΔE and horizontal position signals

Table 2: Event rate and dead-time for various beam currents (electrical) of ^{48}Ti measured in our Faraday cup.

Ibeam (nA)	**Rate (Hz)**	**Dead time (%)**
1.8	170	9
4.4	390	18
8.5	750	29
15.0	1320	42
20.0	1750	49

2.3 Particle identification

A demonstration of the particle identification capabilities of the PSD and FPD was given by the selection of ^{7}Be after the ^{7}Li beam impinged on a target of AlF_3 (this was a test of a future $^{19}F \rightarrow {}^{19}O$ charge exchange reaction, discussed also in Section 3). First a cut (condition) was applied to the $Z = 4$ line in a spectrum of ΔE *vs*. *Er*. Here ΔE is the energy-loss signal in the gas under the 68-mm deep anode section of the ionization chamber, corrected by $\cos(\theta_{foc})$ for the angular variation in track length, and *Er* is the "OR" of any of the (calibrated) silicon energies.

The second step is to select the mass by applying a condition to a matrix of TOF *vs*. X_{foc} (gated by $Z = 4$), where the TOF is the time difference between the PSD and the silicon detector that triggered the evenet. The final result, passed through the software reconstruction procedure to correct for flight-path differences, is shown in Fig.1.

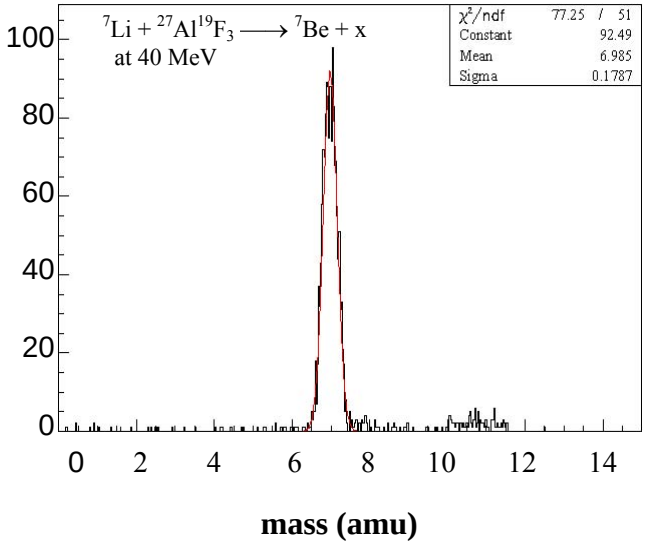

Fig. 1. Reconstructed mass spectrum of ^{7}Be based on TOF gated by a ΔE – Er cut.

2.4 Charge state measurement

The charge state distribution of 120 MeV ^{48}Ti ions elastically scattered from a gold target was measured by taking separate runs with the magnets set to the appropriate rigidity in turn. The integrated counts of the peaks, scaled by the Faraday cup integrated charge and corrected for the acquisition dead time are plotted in Fig. 2. They are in good agreement with predictions of algorithms taken from the code INTENSITY [5].

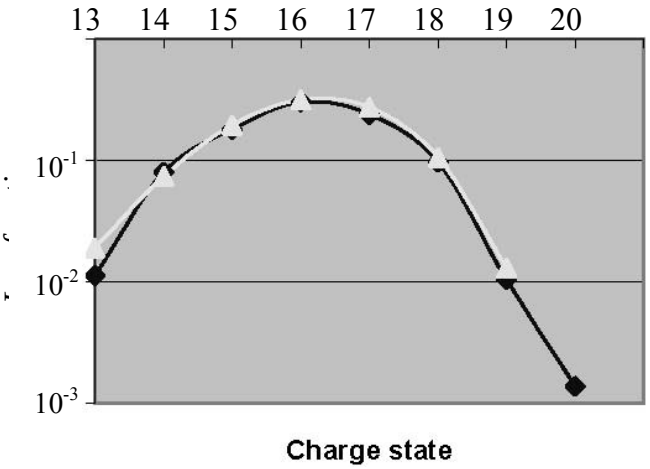

Fig. 2. Charge state distribution of scattered 120 MeV ^{48}Ti ions. Diamonds: measurements by MAGNEX. Triangles: predictions by algorithms from ref. [5].

3 ANGLE AND POSITION (EXCITATION ENERGY) SPECTRA

The horizontal position X_{foc} in the FPD is taken from the drift chamber (DC) closest to the gas window. The vertical position Y_{foc} is obtained from the drift time of the electrons. The horizontal and vertical angles, θ_{foc} and φ_{foc}, are calculated from the first and subsequent DCs. Normally, the initial vertical angle φ_i is taken directly from the PSD. For the initial commissioning this was not implemented, so φ_i had to be reconstructed from φ_{foc}. Because of the small φ_{foc}/φ_i, the reconstruction of φi from is compromised by straggling and detector resolution [2].

The software reconstruction [6] to obtain the initial (scattering) angle and energy uses the COSY INFINITY program [7] to calculate the transport matrices and their inverses. Although it was not available at the time of the experiment, the complicated 3D-interpolation of the maps of the measured fields is now complete and we are able to use realistic fringe fields in the reconstruction. This analysis is still in progress. Nevertheless, the preliminary results are encouraging: see the reconstructed θ_i spectrum shown in Fig. 3. For this measurement an aperture with 1 mm diameter holes was mounted after the target; the horizontal separation between holes subtending 73 mrad. The width of the first peak in the figure is consistent with the size of the holes.

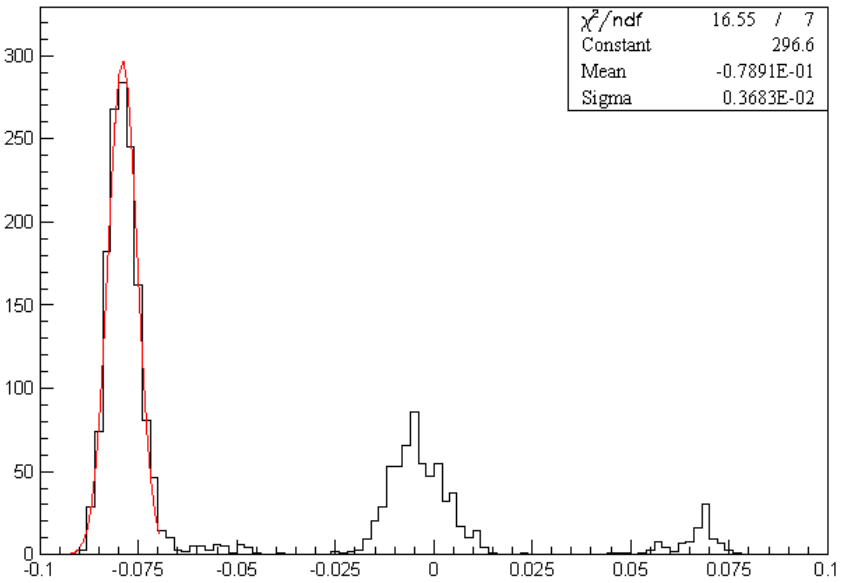

Fig 3: Reconstructed θ_i spectrum for ^{16}O scattered from ^{58}Ni. An aperture with 1 mm holes was located after the target.

To check the momentum dispersion of the spectrometer, two measurements of X_{foc} were made with the same magnet settings but with the energy of the ^{48}Ti beam from the Tandem changed by a few percent. After adjusting the energies for the loss in the target and PSD foil, we obtained a dispersion of 3.68 cm/% for a K of -0.104, which agrees well with the ion optical design.

Figure 4 shows a comparison between the focal plane position spectrum X_{foc} and the reconstructed excitation energy spectra *Exc* for the ^{19}F(^{7}Li,^{7}Be)^{19}O charge exchange reaction mentioned in Section 3. The doublet near 1.5 MeV in *Exc* corresponds to the ground state of ^{19}O with the ejectile ^{7}Be in its ground and 0.429 MeV excited state (there also may be the unresolved 96 keV state of ^{19}O contributing to both ^{7}Be peaks). In the X_{foc} spectrum the doublet is not resolved. Because of the large scattering angle, as well as the PSD (3.5 μm) and FPD gas-window (6 μm) foil thicknesses − both of which were much thicker than would be used in the actual experiment − the resolution obtained does not reflect the true capabilities of the spectrometer (the energy-loss in the PSD foil as well as that in the target explains why the ground state of ^{19}O is not at 0 MeV, since those effects were not included in the reconstruction). The figure is intended only as a preliminary indication of the potential of the ray reconstruction procedure.

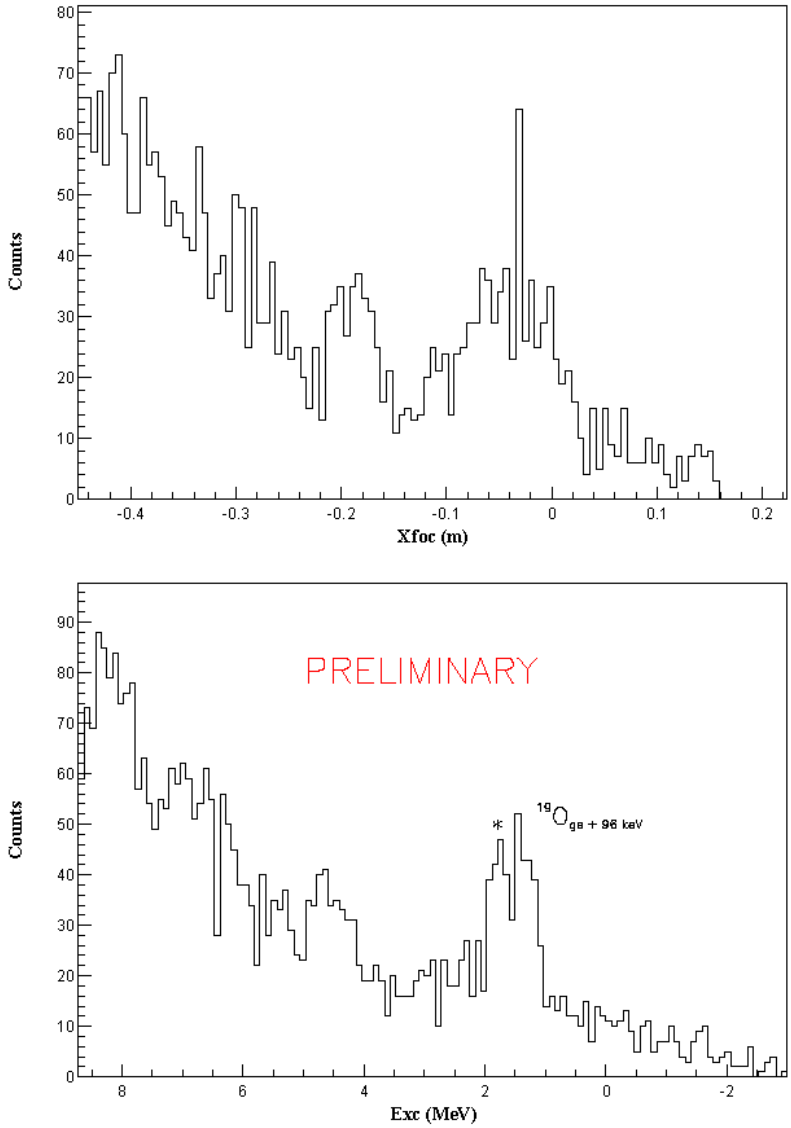

Fig 4. Focal plane position spectrum (top) and software-reconstructed excitation energy spectrum (bottom) for the (^{7}Li, ^{7}Be) charge-exchange reaction on an AlF_3 target. The peak marked with an asterisk is associated to the ejectile in its 0.429 MeV excited state.

REFERENCES

[1] A.Cunsolo et al., Nucl. Instr. Meth. A 481 (2002) 48.

[2] A.Cunsolo et al., Nucl. Instr. Meth. A 484 (2002) 56.

[3] A.Cunsolo et al., LNS Activity Report 2004, p. 113.

[4] A.Cunsolo et al., Nucl. Instr. Meth. A495 (2002) 216.

[5] J.A.Winger et al., Nucl. Instr. Meth. B 70 (1992) 380.

[6] A.Lazzaro et al., Proc. of the 7th Int. Computational Accelerator Physics Conf., East Lansing, Michigan, Oct. 2002 (M. Berz and K. Makino, eds.) IOP conf. series 175 (2005) p.171.

[7] M.Berz and K.Makino, COSY INFINITY version 8.1.